MODELLING OF INVERSION PROCESSES AND CLOUD-TOP ENTRAINMENT

M.K. MacVean
U.K. Meteorological Office
Bracknell, England

1. INTRODUCTION

According to a recent global climatology, the atmospheric boundary layer contains cloud about 60% of the time, with stratus or stratocumulus being the most commonly reported cloud type. Such cloud is very important both for climate and local weather because of its effect on the radiation budget. Cloud-capped boundary layers are generally characterized by strong gradients in temperature and humidity across cloud top. A good understanding of the mixing processes across cloud top is crucial to accurate modelling of such boundary layers. Unfortunately, several difficulties stand in the way of such understanding.

Figure 1 illustrates that the typical vertical scale of variation of properties across the inversion is very small (typically of order $1–10m$) compared to the boundary layer depth or the scale of the large eddies. Longwave radiative cooling near cloud top has a comparably small vertical scale. As a result it is very difficult both to obtain good observations and to model numerically the range of scales involved. Also great care is needed in the choice of numerical methods for modelling, in order to accurately simulate the advection of sharp gradients and changes of gradient.

Measurement and modelling of the cloudy boundary layer is thus a particularly challenging problem and it is a very active area of research with ongoing controversy, particularly as regards cloud-top entrainment instability. The current state of the art as regards simulation using fine-scale models can be summarized as follows. Unequivocal "direct" simulations are not feasible, even if one allows the term "direct simulation" to include models with a constant eddy viscosity which is significantly greater than the molecular viscosity, although still small. Optimistically one might require a grid spacing of order $10cm$ in a domain with linear dimensions of order $1km$ for such a simulation. Even two-dimensional simulations with such parameters are unlikely to be feasible for some time to come, while corresponding three-dimensional simulations (which are what is really required) will remain impractical for the foreseeable future. On the other hand, large-eddy

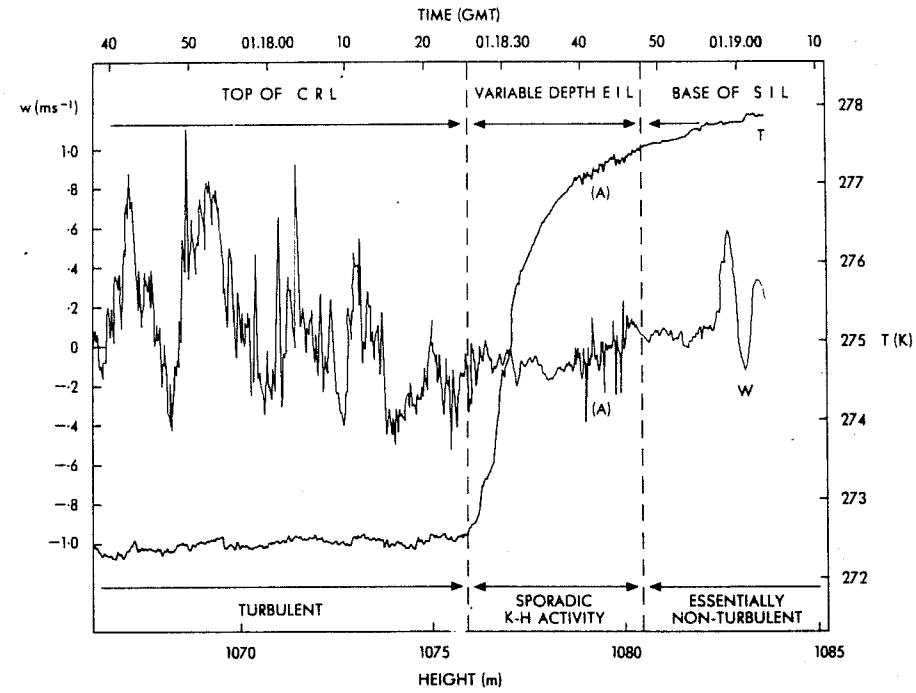

Fig 1: High resolution profiles of the vertical velocity and temperature fields across the top of a stratocumulus deck, from Caughey et. al. (1985)

simulations have already been carried out in two-dimensions, with a resolution of a few metres and in three-dimensions with grid spacings of a few tens of metres. Since such simulations include a subgrid model, involving assumptions and choices of parameters which are not easily verified, because of the lack of appropriate turbulence data, caution must be exercised in the use of data from such simulations as a proxy for observational data.

In this paper, we will first consider two issues of relevance to large-eddy simulation of the cloudy boundary layer, namely the choice of numerical scheme and the parametrization of the subgrid buoyancy flux. The latter leads naturally on to a discussion of cloud-top entrainment instability, after which two outstanding issues with regard to parametrization of such boundary layers in large-scale models are briefly considered.

2. NUMERICAL SCHEMES FOR ADVECTION

It is well known that many simple advection schemes (for example, second-order centred differences) handle the advection of sharp gradients or changes of gradient poorly, developing spurious oscillations of quite large amplitude. This is a particularly serious problem

in models of the cloud-capped boundary layer, which is characterized by a very sharp transition from the well-mixed cloud layer to the strongly stratified inversion. Energetic eddies within the boundary layer may cause vertical displacements of the inversion, if they extend to cloud top, and if inadequate numerical schemes are used, unphysical behaviour is observed. Typically, a spurious, relatively dry layer forms at the top of the inversion. Instantaneously, negative humidities may occur at some grid points. The behaviour at the base of the inversion is somewhat different, as the overshoots tend to be quickly mixed over the whole layer, resulting in a spurious moistening. Similar effects are observed in the temperature field; the combined effect on the buoyancy field is such as to generate regions of static instability above cloud top, which feed back through the subgrid model and can result in the formation of a spurious mixed layer at the top of the inversion. Clearly there is little point in worrying about the realism of any subgrid model close to cloud top, in the presence of such numerical effects. The development of numerical schemes which do not exhibit such behaviour is an area of active research. It must be remembered that the avoidance of overshoots in such schemes is generally the result of implicit numerical diffusion in some form. In choosing an algorithm, it is important to check that this diffusion is acceptably small. Otherwise there is the risk that one is merely exchanging one set of problems for another. In the light of extensive experimentation with various schemes in our model of the stratocumulus-capped boundary layer at the UK Met. Office, we feel that the approach of Leonard (1991) and, in particular, his ULTIMATE QUICKEST scheme, has much to recommend it, being simple, robust and effective.

3. SUBGRID BUOYANCY FLUX

A key element in the formulation of most subgrid models is the parametrization of the buoyancy flux. In first-order closures, this is required as the numerator for the Richardson Number; in closures involving an equation for turbulent kinetic energy, it appears on the right-hand side of that equation. In many models, this quantity is required at the centre of the top and bottom faces of control volumes centred on the grid points at which the thermodynamic variables are held. When two vertically adjacent control volumes are either both saturated or both unsaturated, the calculation of the buoyancy flux on the interface between them, in terms of the fluxes of conservative variables is straightforward. However, the formulae are quite different in the two cases and the crucial question which arises is how the case when one control volume is saturated and the other unsaturated

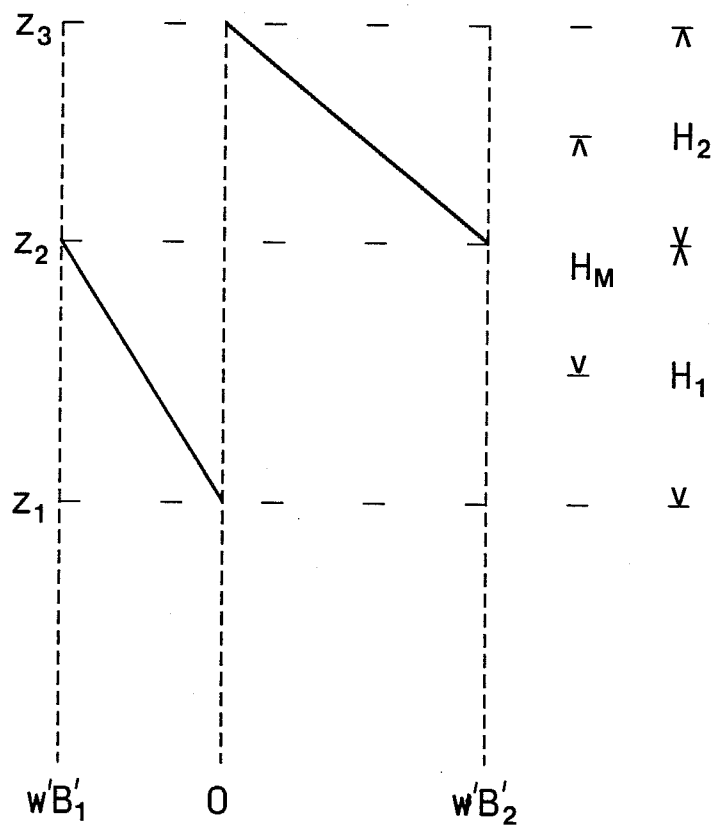

Fig. 2: The buoyancy flux profile assumed to result from the specified mixing process

should be treated. It is not generally clear from the descriptions in the literature how this case is dealt with in particular closures. Where this case is addressed, the normal approach appears to be to take a weighted mean of the formulae for the saturated and unsaturated cases. Great care needs to be taken if such an approach is to be energetically consistent. An alternative approach, which is guaranteed to be energetically consistent, was first proposed by Mason (1985) and further developed by MacVean and Mason (1990).

MacVean and Mason's approach treats two adjacent control volumes as a thermodynamically closed system and considers the energetic implications of exchanging an arbitrary, small volume of fluid between the two, initially homogeneous layers and then rehomogenizing them. The assumption is made that any change of state and associated latent heat change occurs instantaneously and at the interface. Consistent with this, the buoyancy flux resulting from this exchange is modelled as shown in Fig.2.

It is easily shown that the total buoyancy flux within the system is related to the net conversion from kinetic to potential energy (S) by

$$-\frac{\partial}{\partial t}\int_{z_1}^{z_3}\overline{K}dz = S = -\int_{z_1}^{z_3}\overline{w'B'}dz$$

where $\overline{K}$ is the resolved kinetic energy. Given our assumption about the location of the latent heat release, B may be treated as a conserved quantity *within each layer individually* and therefore satisfies

$$\left(\frac{\partial\overline{B}}{\partial t}\right)_1 = -\left(\frac{\partial\overline{w'B'}}{\partial z}\right)_1 = -\frac{(\overline{w'B'})_1}{H_1}$$
$$\left(\frac{\partial\overline{B}}{\partial t}\right)_2 = -\left(\frac{\partial\overline{w'B'}}{\partial z}\right)_2 = +\frac{(\overline{w'B'})_2}{H_2}$$

where $(\overline{w'B'})_1$, $(\overline{w'B'})_2$ are the values of the buoyancy flux at the top of the lower layer and the bottom of the upper layer, respectively. Given the assumed linear variation of buoyancy within the layers, it can be shown that

$$S = -\int_{z_1}^{z_3}\overline{w'B'}dz = \frac{\partial P}{\partial t}$$

where P, the time-varying part of the total potential energy relevant to the specified mixing process is defined by

$$P = (\overline{B}_1{H_1}^2 - \overline{B}_2{H_2}^2)/2$$

If we discretize over the time δt taken for the small volume ϵH_2 to be exchanged and introduce the depth-averaged buoyancy flux $\overline{w'B'}_{AV}$, then we obtain

$$(H_1+H_2)\overline{w'B'}_{AV} = -\frac{\delta P}{\delta t} = -\eta\frac{\delta P}{\epsilon H_2} \tag{1}$$

Here, $\eta = \epsilon H_2/\delta t$ is the rate at which volumes of material are exchanged between the layers.

We will now outline how this energetically consistent formulation of the buoyancy flux may be used in first- or second-order closures. In the framework of a K-theory local turbulence closure, η may be related to an eddy viscosity ν_I at the interface, by $\eta = \nu_I/H_m$ where $H_m = (H_1+H_2)/2$. Then, denoting by an asterisk superscript, values of quantities after the specified mixing process has occurred, we may write

$$\overline{w'B'}_{AV} = \frac{\nu_I[(\overline{B}_2^* - \overline{B}_2){H_2}^2 - (\overline{B}_1^* - \overline{B}_1){H_1}^2]}{\epsilon H_2(H_1+H_2)^2} \tag{2}$$

The buoyancy is determined from the appropriate conserved variables through a constitutive relationship, while the values of any conserved variable C after mixing are given by

$$\overline{C}_2^* = (1-\epsilon)\overline{C}_2 + \epsilon\overline{C}_1 \tag{3}$$

$$\overline{C}_1^* = (1-\epsilon\frac{H_2}{H_1})\overline{C}_1 + \epsilon\frac{H_2}{H_1}\overline{C}_2 \tag{4}$$

For a linear constitutive relationship, assuming that ϵ is so small that the mixing does not change the states of saturation of the layers, the buoyancy flux may be shown to be independent of ϵ when (2) is expressed in terms of conserved variables. Furthermore, in the cases where either both layers are saturated or both are unsaturated, and therefore there is no discontinuity in the buoyancy flux at the interface, it may be shown that

$$\overline{w'B'}_I = 2\overline{w'B'}_{AV} = -\nu_I(\overline{B}_2 - \overline{B}_1)/H_m$$

Thus, in this case, our scheme reduces to the standard K-theory definition of the buoyancy flux.

For a fixed Prandtl Number, a Richardson Number (Ri) can be calculated from (2) and the resolved deformation (χ^2), without prior knowledge of ν_I. The eddy viscosity can then be calculated from a general mixing length closure, which takes the form $\nu_I = \ell^2\chi(1-Ri)^{1/2}$, where the length scale ℓ is a function of Ri and perhaps other factors. Once ν_I has been determined, the turbulent fluxes of conservative properties between the layers can be estimated using K-theory.

In a second-order closure, predictive equations are carried for the subgrid fluxes of conserved variables. The divergence of these fluxes can be used instead of (3) and (4) to determine the implied new values of the conserved variables. These may, in turn, be used to calculate δP, from which $\overline{w'B'}_{AV}$ may be calculated, using the left-hand equality in (1). This value of the subgrid buoyancy flux is then used in the equation for the vertical velocity variance. An independent choice of parametrization for this flux is likely to be energetically inconsistent.

In deriving the parametrization above, we have considered carefully the energetics of mixing across cloud top. It was realized many years ago that, under certain circumstances, evaporative cooling resulting from such mixing could lead to the formation of saturated air parcels which were denser than the undisturbed cloudy environment. Randall (1980)

and Deardorff (1980) independently derived criteria for this to occur. It was also postulated that the sinking of the dense air parcels away from cloud top could lead to further mixing across cloud top, constituting a positive feedback mechanism, which might lead to the rapid breakup of stratocumulus sheets. This process became known as cloud-top entrainment instability. As a criterion for buoyancy reversal (the generation of mixtures denser than either of the components), Randall and Deardorff's condition is generally accepted. It can be expressed in terms of the jumps across cloud top of equivalent potential temperature ($\Delta\overline{\theta}_e$) and total water mixing ratio ($\Delta\overline{q}_t$) as

$$\Delta\overline{\theta}_e < k_w \frac{L}{c_p} \Delta\overline{q}_t \tag{5}$$

where k_w is a function of state, having a typical value of 0.23. However, its relevance to the rapid breakup of stratocumulus has been increasingly questioned as more observational data has become available. Figure 3 shows data compiled by Kuo and Schubert (1988); it may be seen that there are about as many observations of persistent stratocumulus on either side of the line BO, which represents Randall and Deardorff's stability boundary. MacVean and Mason (1990) and Siems et al (1990) have both suggested that Randall and Deardorff's analysis does not address the crucial requirement for a direct feedback process, namely that there be a net kinetic energy release due to the postulated initial mixing, *on the same space- and time-scales as that mixing.* Their analysis also neglects the work done against gravity in entraining the less dense, unsaturated air into the cloud. MacVean and Mason argue that, provided one considers two layers of approximately equal thickness, comparable to the scale of entrainment across cloud top (a metre or so, say), then the model already presented for determining the subgrid buoyancy flux in a turbulence closure, embodies the condition for the existence of the direct feedback mechanism which is called cloud-top entrainment instability. Under the above assumptions, if $S < 0$ then the specified initial small amount of mixing results in an increase in the net kinetic energy on the time and space scales of that initial mixing. This condition can be expressed as

$$\Delta\overline{\theta}_e < k_m \frac{L}{c_p} \Delta\overline{q}_t \tag{6}$$

where k_m is a function of state with a typical value of 0.7. It may be seen from Fig.3 that this stability boundary delimits quite well the region of parameter space in which persistent stratocumulus is observed. However, there is very little data from the situations when

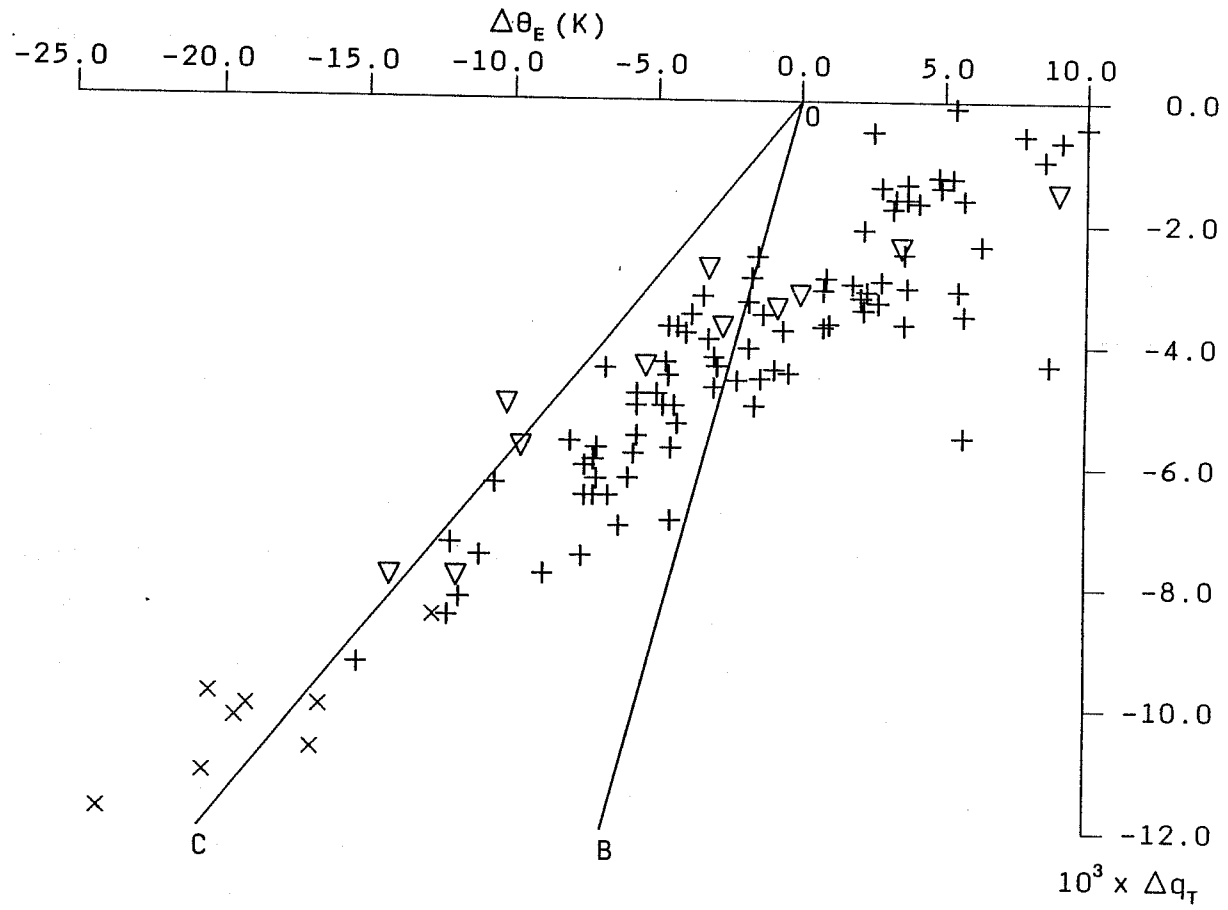

Fig. 3: Data on the jumps in properties across cloud top, as assembled from various sources by Kuo and Schubert (1988). The symbol + indicates an observation of persistent stratocumulus, Δ an observation of stratocumulus which subsequently broke up within 12*h* and x and observation of trade-wind cumulus. Also shown are the stability boundaries *BO* and *CO* corresponding to (5) and (6), respectively.

stratocumulus is rapidly breaking up, which are crucial for the verification of any criterion. Betts and Boers (1990) have, however, analysed data obtained across a cloudiness transition during FIRE. They identified four regimes—stratocumulus (99% cloud cover), broken (73%), cumulus (12%) and clear (0%). We have calculated corresponding values of the stability parameter $R = \Delta\bar{\theta}_e/(L/c_p)\Delta\bar{q}_t$ as 0.34, 0.53, 0.69 and 0.72. This data is therefore consistent with the relevance of (6) rather than (5) to cloud-top entrainment instability.

It is hoped that forthcoming experiments such as ASTEX will provide better data for examining the validity of criteria for stratocumulus breakup. In the meantime, an extensive programme of numerical experimentation has been carried out using a two-dimensional version of our large-eddy model. A domain $2.5km$ wide and $4km$ deep was considered, using a uniform horizontal grid length of $5m$ and a vertical grid with a uniform spacing of $5m$ for a few hundred metres either side of cloud top, although non-uniform and coarser elsewhere. In order to isolate the effect of entrainment across cloud top, surface fluxes and radiative parametrizations were not included. The model was initialized with a horizontally homogeneous initial state on which was superimposed a random humidity perturbation of very small amplitude at a single level about $100m$ below cloud top. The cloud extended from about $650m$ to $1100m$ and had a maximum liquid water mixing ratio of $0.8gkg^{-1}$. The initial conditions above cloud top were carefully chosen to ensure that the horizontal mean value of the stability parameter R remained very close to the value initially specified, throughout the integration. The initial conditions below cloud top and the complete initial buoyancy profile were the same for all runs. Integrations were carried out for a range of values of R. It was also judged to be of crucial importance to determine the sensitivity of our results to the subgrid model employed. Subgrid models employed included the first-order closure detailed earlier in this paper (referred to as MM), several variants thereof and several constant values of eddy viscosity.

Figure 4 shows timeseries of the domain-integrated liquid water content at various values of R from integrations using the subgrid model MM. It must be remembered that with this subgrid model there is no explicit mixing across cloud top for $R < 0.7$. It may be seen that when there is small-scale turbulent mixing across cloud top ($R = 0.78$), the cloud breaks up very rapidly—a typical e-folding decay scale over the period from 1800s–5400s is about $700s$. Within the 90 minutes following initialization with an extremely

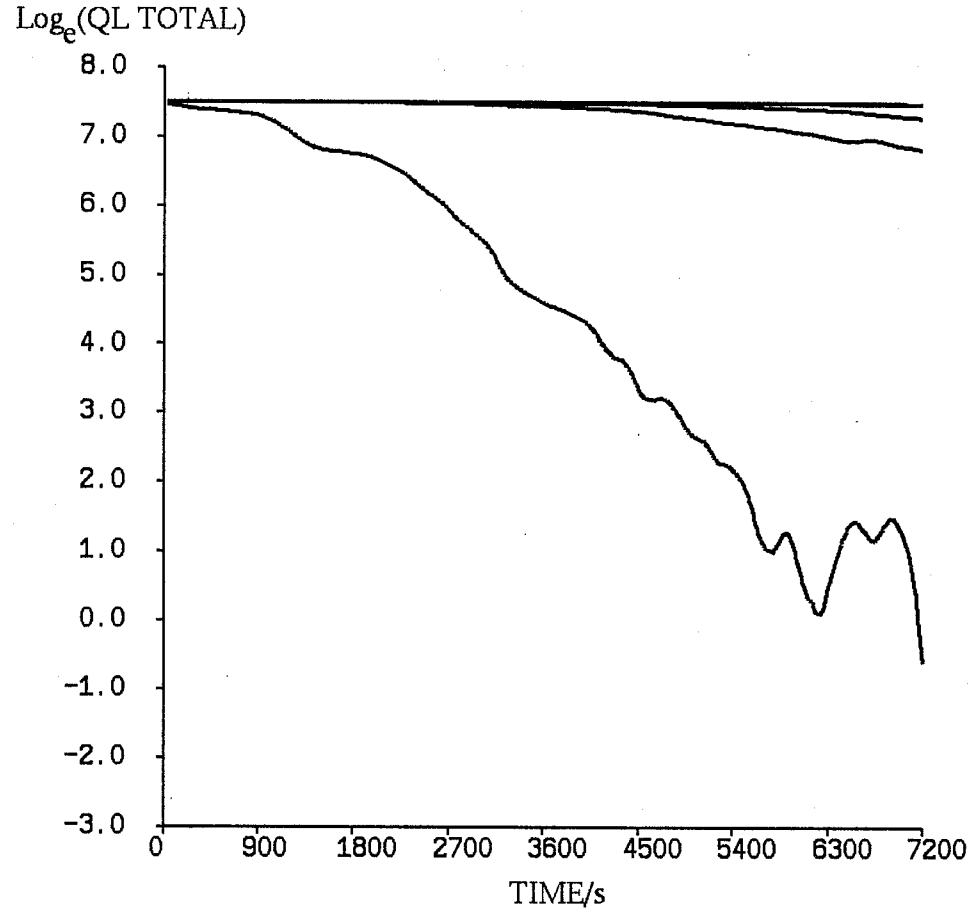

Fig. 4: Timeseries of the domain-integrated liquid water content from integrations using subgrid model *M M*, at R = 0.78 (lowest curve), 0.6, 0.5, 0.4, 0.3 and 0.18 (uppermost curve)

small perturbation, the total liquid water content has dropped to less than 1% of its initial value, with a cloud cover of less than 20%.

For $R < 0.23$ buoyancy reversal does not occur and so there is no source of kinetic energy in the model. Accordingly, the cloud field remains essentially horizontally homogeneous and there is no perceptible decline in the total cloud amount. For $0.7 > R > 0.23$ buoyancy reversal does occur, as a result of the implicit diffusion of the numerical advection scheme. The kinetic energy generated increases with R but even at $R = 0.6$ there is no evidence that it leads to runaway entrainment. Over the first two hours, the horizontal homogeneity of the cloud is destroyed and very occasional breaks occur in it but the cloud cover remains in the range 95–100%.

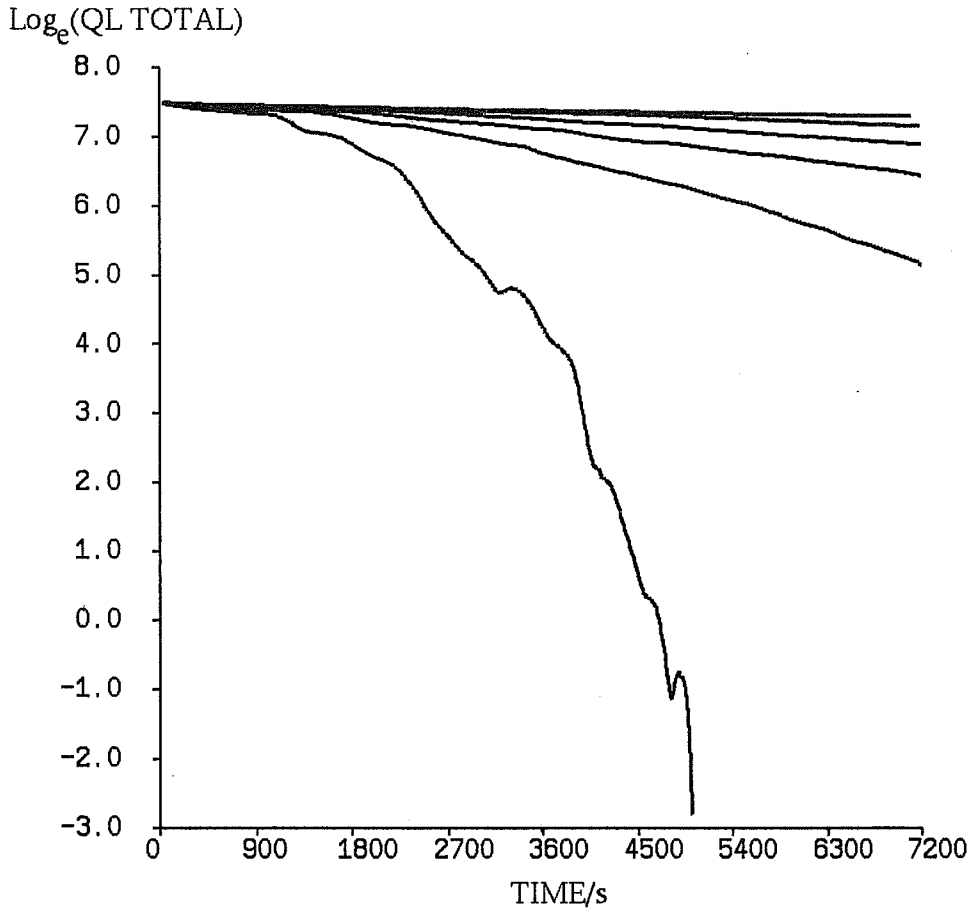

Fig. 5: As Fig. 4 but for integrations with a constant eddy viscosity of $0.2m^2s^{-1}$

Figure 5 shows corresponding timeseries from integrations with a constant eddy viscosity of $0.2m^2s^{-1}$. The e-folding decay scale for $R = 0.78$ (measured from 1800–3600s) is of order 600s, which is comparable to that seen previously. The cloud has completely disappeared in less than 90 minutes. The constant eddy viscosity leads to a slow decline in liquid water, even for $R = 0.18$. However, in that case the cloud remains essentially horizontally homogeneous. For $R > 0.23$ the horizontal homogeneity is again destroyed as a result of the buoyancy reversal. The e-folding decay time increases with R but at $R = 0.6$ it is still about 3000s, some 5 times longer than for $R = 0.78$. For $R = 0.6$ the cloud thins significantly over the two hour period shown but relatively few breaks occur in it, the cloud cover still exceeding 90% at the end.

Figure 6 shows timeseries from integrations with $R = 0.78$, using various different subgrid models. Only a weak dependence on the subgrid model is apparent. In each case,

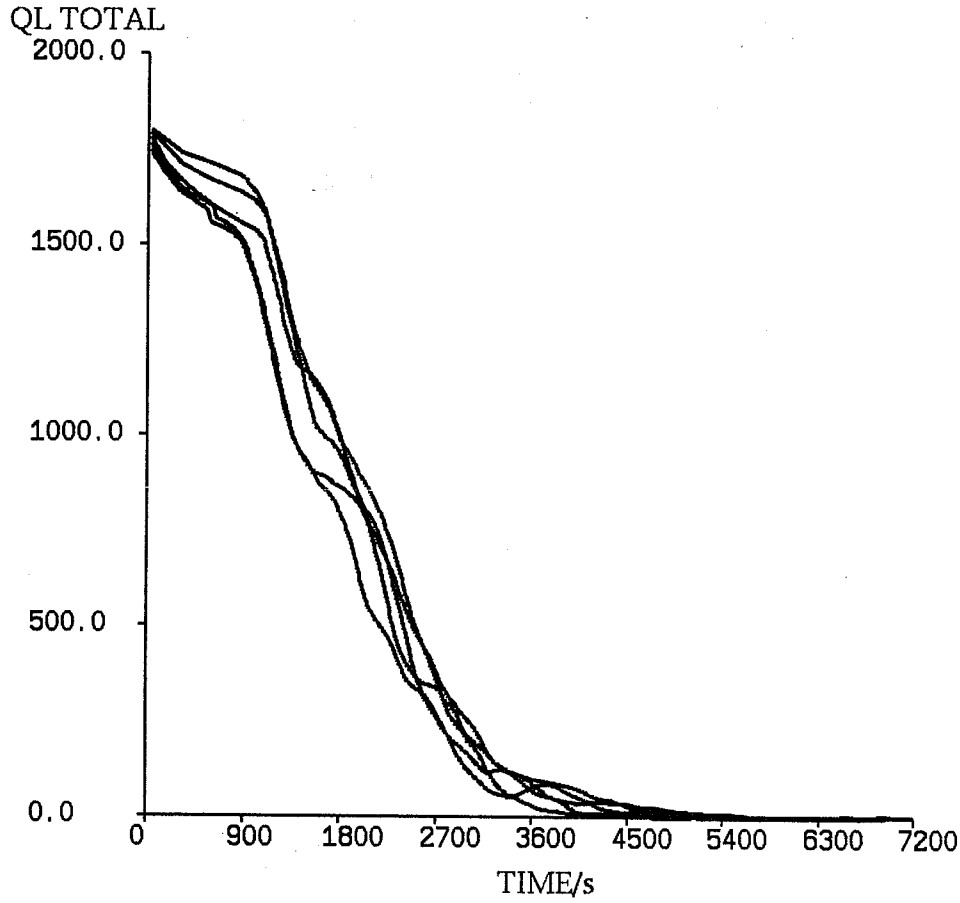

Fig. 6: Time series of the domain-integrated liquid water content for integrations at $R = 0.78$ with various subgrid models

the cloud dissipates so quickly (with an e-folding time of typically $600 - -700s$) that it is hard to conceive of any process for replenishing moisture which could act rapidly enough to stop the cloud evaporating completely within an hour or two. On the other hand, for values of R just above the critical value for cloud-top entrainment instability suggested by Randall and Deardorff, there is no sign of runaway entrainment. Convective motions driven by the buoyancy reversal disrupt the horizontal homogeneity of the initial state but the cloud cover remains close to 100% and the decline in the liquid water occurs at such a slow rate that it might well be reversed if moisture sources were included.

Figure 7 shows a plot of the decay rates against R from integrations with various subgrid models. These graphs are characterized by an almost linear increase with R from the buoyancy reversal criterion ($R = 0.23$) up to about $R = 0.5$ and a very rapid increase

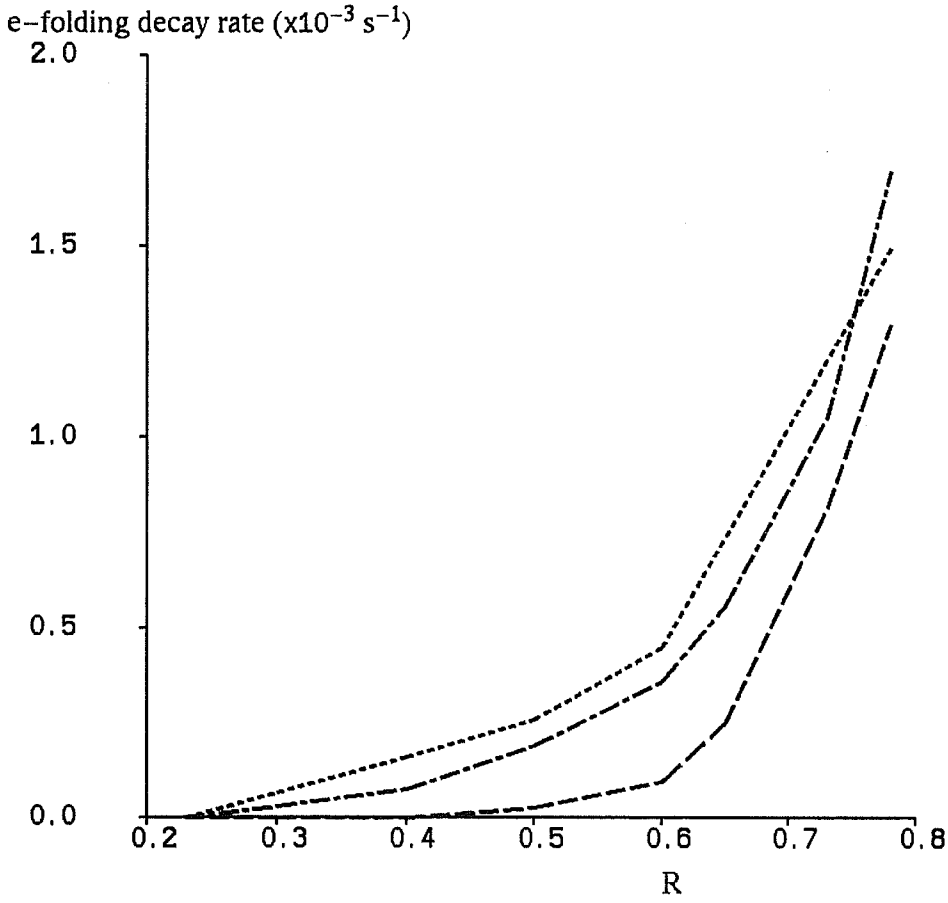

Fig. 7: Variation of the e-folding decay rate with R from integrations with various subgrid models

between $R = 0.6$ and $R = 0.78$.

These results strongly suggest that cloud-top entrainment instability may be a very potent mechanism for the breakup of stratocumulus cloud but that it does not occur at the point in parameter space suggested by Randall and Deardorff but rather, at values close to the critical one derived by MacVean and Mason. We have considered cloud-top entrainment alone in this study and deliberately excluded other physical processes such as radiation and surface fluxes, which may play a significant role in reality. Our results should therefore be interpreted as indicating that it is highly unlikely that stratocumulus will persist at values of R in excess of about 0.7 *not* that stratocumulus *will* persist at lower values of R. Processes other than, or in addition to, cloud-top entrainment could well lead to breakup in this region of parameter space.

4. PARAMETRIZATION IN LARGE-SCALE MODELS

A subgrid parametrization equivalent to MM has been included in the UKMO atmospheric GCM (Smith,1990). Such an application raises two issues in particular, which merit further consideration.

In the large-eddy model used in the studies reported here, the convective motions resulting from buoyancy reversal if $R > 0.23$, occur mainly on the resolved scale and it is only the mixing on a scale of a few metres or less (which leads to the buoyancy reversal), which is parametrized. The convective motions which are resolved in the large-eddy model, become subgrid-scale in a GCM but a parametrization such as MM clearly does not represent them. The question is whether this upside-down convection is represented by another parametrization in the GCM and, if not, whether this is a serious omission.

The second issue concerns the interpretation of the MM subgrid model when applied on a GCM grid. Typically the vertical grid spacing close to cloud top will be at least several hundred metres and, moreover, the thickness of the layer just above cloud top may be significantly greater than that of the layer immediately below. Thus the conditions which were previously argued to be necessary for the MM closure to embody the condition for existence of a direct feedback mechanism do not appear to be satisfied. Also, MacVean and Mason have shown that the critical value of R at which the conversion from potential to kinetic energy changes sign is, in general, a function of the ratio of the layer thicknesses. If the layer thickness increases significantly with height across cloud top, as in many GCMs, then the critical value of R is increased from 0.7 towards 0.93, the value for static instability in an unsaturated atmosphere. Thus it would appear to be artificially harder to initiate subgrid mixing across cloud top with such a grid configuration. One might expect this to result in a tendency for over-persistence of stratocumulus layers. However, Smith reports that this is not the case in his GCM simulations and suggests that the penetrative convection scheme may compensate for the reduction in diffusive mixing.

5. REFERENCES

Betts, A.K. and R. Boers, 1990: A cloudiness transition in a marine boundary layer. *J. Atmos. Sci.*, **47**, 1480–1497.

Caughey, S.J., B.A. Crease and W.T. Roach, 1985: A field study of nocturnal stratocumulus. II: Turbulence structure and entrainment. *Quart. J. Roy. Meteor. Soc.*, **109**, 124–144.

Deardorff, J.W., 1980: Cloud-top entrainment instability. *J. Atmos. Sci.*, **37**, 131–147.

Kuo, H., and W.H. Schubert, 1988: Stability of cloud-topped boundary layers. *Quart. J. Roy. Meteor. Soc.*, **114**, 887–916.

Leonard, B.P., 1991: The ULTIMATE conservative difference scheme applied to one-dimensional advection. *Computer Methods in Applied Mechanics and Engineering*,**88**, 17–74.

MacVean, M.K., and P.J. Mason, 1990: Cloud-top entrainment instability through small-scale mixing and its parametrization in numerical models. *J. Atmos. Sci.*, **47**, 1012–1030.

Mason, P.J., 1985: A numerical study of cloud streets in the planetary boundary layer. *Bound. Layer Meteor.*, **32**, 281–304.

Randall,D.A., 1980: Conditional instability of the first kind upside-down. *J. Atmos. Sci.*, **37**, 125–130.

Siems, S.T., C.S. Bretherton, M.B. Baker, S. Shy and R.T. Breidenthal, 1990: Buoyancy reversal and cloud-top entrainment instability. *Quart. J. Roy. Meteor. Soc.*, **116**, 705–739.

Smith, R.N.B, 1990: A scheme for predicting layer clouds and their water content in a general circulation model. *Quart. J. Roy. Meteor. Soc.*, **116**, 435–460.